A 106-kDa Aminopeptidase Is a Putative Receptor for *Bacillus thuringiensis* Cry11Ba Toxin in the Mosquito *Anopheles gambiae*[†]

Rui Zhang,[‡] Gang Hua,[‡] Tracy M. Andacht,[§] and Michael J. Adang*[,‡,||]

Departments of Entomology and Biochemistry and Molecular Biology and Proteomics and Mass Spectrometry Facilities, University of Georgia, Athens, Georgia 30602-2603

Received June 24, 2008; Revised Manuscript Received September 3, 2008

ABSTRACT: *Bacillus thuringiensis* (Bt) insecticidal toxins bind to receptors on midgut epithelial cells of susceptible insects, and binding triggers biochemical events that lead to insect mortality. Recently, a 100-kDa aminopeptidase N (APN) was isolated from brush border membrane vesicles (BBMV) of *Anopheles quadrimaculatus* and shown to bind Cry11Ba toxin with surface plasmon resonance (SPR) detection [Abdullah et al. (2006) *BMC Biochem. 7*, 16]. In our study, a 106-kDa APN, called AgAPN2, released by phosphatidylinositol-specific phospholipase C (PI-PLC) from *Anopheles gambiae* BBMV was extracted by Cry11Ba bound to beads. The AgAPN2 cDNA was cloned, and analysis of the predicted AgAPN2 protein revealed a zinc-binding motif (HEIAH), three potential *N*-glycosylation sites, and a predicted glycosylphosphatidylinositol (GPI) anchor site. Immunohistochemistry localized AgAPN2 to the microvilli of the posterior midgut. A 70-kDa fragment of the 106-kDa APN was expressed in *Escherichia coli*. When purified, it competitively displaced ^{125}I-Cry11Ba binding to *An. gambiae* BBMV and bound Cry11Ba on dot blot and microtiter plate binding assays with a calculated K_d of 6.4 nM. Notably, this truncated peptide inhibited Cry11Ba toxicity to *An. gambiae* larvae. These results are evidence that the 106-kDa GPI-anchored APN is a specific binding protein, and a putative midgut receptor, for Bt Cry11Ba toxin.

The mosquito, *Anopheles gambiae*, is the principal vector of *Plasmodium falciparum* that causes human malaria. *Anopheles* species are typically controlled at the adult stage by chemical pesticides. Depending on the larval habitat, treatment with *Bacillus thuringiensis* (Bt)[1] biopesticides, however, can have an important role in vector management programs (*1, 2*).

Insecticidal Cry toxins recognize receptor molecules located in the brush border of target insects. In lepidopteran larvae, the Cry1 toxins bind cadherins, aminopeptidases (APN), alkaline phosphatase (ALP), and glycolipids. According to proposed models for toxin action (reviewed in ref *3*), binding to multiple receptors is required to induce toxin processing, prepore formation, and membrane insertion (*4*).

The Cry4 and Cry11 toxins of Bt *israelensis* bind to the apical microvilli of midgut cells in gastric ceca and posterior midgut of mosquito larvae (*5−8*). A 65-kDa protein binds Cry4Ba and Cry11Aa in *Aedes* larvae (*9*). The 65-kDa protein was identified as an ALP and confirmed as a Cry11Aa receptor (*10*). Recently, the AgCad1 cadherin from *An. gambiae* was identified as a binding protein and putative receptor for Cry4Ba toxins (*11*).

APNs are exoenzymes located in the brush border of insect larvae. Lepidopteran larvae have at least four paralogues of APN located on the surface of their midgut brush border membrane. Presumably, the different APNs have cleavage preferences for various classes of amino acids. These molecules also function as adventitious receptors for Bt Cry1 toxins. In the mosquito *Anopheles quadrimaculatus*, a 100-kDa APN (APN$_{Anq}$100) has tight binding to Cry11Ba but not to Cry11Aa or Cry4Ba toxin according to binding analysis by SPR (*12*).

In the present study, we describe the cloning and identification of an APN-like protein from the gut of *An. gambiae*. Immunohistochemistry study shows that the APN localizes on the apical cell membrane in the posterior midgut of the mosquito. Binding studies using APN released from BBMV of the mosquito larvae and *Escherichia coli* cell-expressed truncated APN peptide are evidence that the protein is a Cry11Ba binding protein. Bioassays using the truncated peptide display an inhibition effect with Cry11Ba, which provide further evidence that the APN is a Cry11Ba receptor. This is the first report of an APN-type protein as a Cry toxin binding protein in *An. gambiae*.

* Address correspondence to this author at the Department of Entomology, University of Georgia. E-mail: adang@uga.edu. Phone: 706-542-2436. Fax: 706-542-2279.
[‡] Department of Entomology, University of Georgia.
[§] Proteomics and Mass Spectrometry Facilities, University of Georgia.
[||] Department of Biochemistry and Molecular Biology, University of Georgia.

[1] Abbreviations: alkaline phosphatase (ALP), aminopeptidase N (APN), *Bacillus thuringiensis* (Bt), brush border membrane vesicles (BBMV), 3-(cyclohexylamino)propanesulfonic acid (CAPS), 3-[(chola-midopropyl)dimethylammonio]-1-propanesulfonate (CHAPS), glyco-sylphosphatidylinositol (GPI), phelylmethanesulfonyl fluoride (PMSF), phosphatidylinositol-specific phospholipase C (PI-PLC), polymerase chain reaction (PCR), and surface plasmon resonance (SPR).

EXPERIMENTAL PROCEDURES

Purification of Cry11Ba Toxin. The Bt strain 407, harboring plasmid pJEG80.1 encoding cry11Ba (*13*), was kindly provided by Dr. D. H. Dean (Ohio Sate University). A complex sporulation medium supplemented with erythromycin antibiotic was used according to ref *14*: 2 g/L peptone (Difco, BD), 5 g/L yeast extract (Difco, BD), 0.07 M K_2HPO_4, 0.02 M KH_2PO_4, 6×10^{-3} M glucose, 2×10^{-4} M $MgSO_4 \cdot 7H_2O$, 5×10^{-4} M $CaCl_2 \cdot 2H_2O$, 6×10^{-6} M $MnSO_4 \cdot 7H_2O$, and 1×10^{-6} M $FeSO_4 \cdot 7H_2O$. The strain was grown in 1 L of media at 30 °C overnight; then 1 L of sodium phosphate solution (0.06 M Na_2HPO_4, 0.04 M $NaH_2PO_4 \cdot H_2O$) was added into the growing culture. Upon completion of sporulation spores and crystals were harvested by centrifugation, resuspended in 0.1 M NaCl, 2% Triton-X 100, and 20 mM Bis-Tris, pH 6.5, sonicated on ice, and then washed in the same buffer three times. The spore−crystal mixture was then washed in 1 M NaCl (twice) and distilled H_2O (twice). All centrifugation steps were 10000*g* for 10 min at 5 °C. Crystals were separated from spores by centrifugation through a 30−60% (w/v) NaBr step gradient at 47000*g* for 2 h at 5 °C. Purified crystals were washed twice with distilled water and dissolved in 100 mM 3-(cyclohexylamino)propanesulfonic acid (CAPS) and 0.05% *β*-mercaptoethanol, pH 10.6, for 2 h at 37 °C, and insoluble material was removed by centrifugation 10000*g* for 10 min. Activation of Cry11Ba protoxin was performed by incubating the toxin with bovine pancreatic trypsin (Sigma) at a mass ratio of 50:1 (toxin:trypsin) for 2 h at 37 °C.

Mosquito Rearing. The colony of *An. gambiae* (CDC G3 strain) was maintained at 27 °C with a photoperiod of 14 h light/10 h dark. Adults were given access to 10% sucrose, and females were fed blood on restrained mice. Fresh eggs were washed with 0.1% bleach and hatched in distilled water. Larvae (ca. 200/pan) were fed with ground TetraMin daily. Larvae were reared to fourth instar, collected, and used immediately for midgut dissection, section preparation, or bioassay.

Midgut Dissection, RNA Isolation, and cDNA Synthesis. The fourth instar larvae were placed in RNAlater (Sigma) for fixation and dissection. The whole intestine, observed under a dissecting microscope, was gently pulled out using a pair of dissecting forceps. The midgut was then isolated by carefully removing the foregut and hindgut and immediately frozen on dry ice, and aliquots of ∼50 mg were stored at −80 °C. Total RNA was extracted from 50 mg of midgut tissue using the RNeasy Mini Kit (Qiagen) according to the manufacturer's instructions. cDNA was synthesized from total RNA using Superscript II reverse transcriptase (Gibco-BRL) and oligo(dT)$_{17}$ primer.

APN cDNA Cloning. Three pairs of specific primers were designed according to the Ensembl gene EN-SANGG00000018740 and used sequentially as shown in Table 1 and Figure 1A. PCR amplifications were performed using synthesized midgut cDNA with 30 cycles of 94 °C for 30 s, 55 °C for 30 s, and 72 °C for 2 or 3 min. The resultant PCR products were cloned into pGEM-T Easy vector (Promega) and sequenced from both forward and reverse directions at the Molecular Genetics Instrumentation Facility (University of Georgia). The cloned 2.9 kb cDNA,

Table 1: Primers Used in This Study

primer	primer sequence (5′−3′)
Primers for Cloning cDNA of AgAPN2	
AgAPN2-F1	5′-ATGACATTGGCAGAAAAGCTAGCGCTG-3′
AgAPN2-R1	5′-GCTAGACTTTATTCATCAATCGTGCTTG-3′
AgAPN2-F2	5′-TTGGCCGCAGTTTAACAACGTTCGGA-3′
AgAPN2-R2	5′-GCCACATTCGTGTAACTACCGTGCG-3′
AgAPN2-F3	5′-TGGCCGCGGTACCTGATTTCTCTG-3′
AgAPN2-R3	5′-TCAGGATCTGCTCTGTCGCCACGTT-3′
Primers for Cloning APN2$_t$	
AgAPN2-F4	5′-CGCACATATGGGCCGCAGTTTAACAA-3′
AgAPN2-R4	5′-AGGCCTCGAGCACATTCGTGTAACTA-3′

designated *AgAPN2*, contains an open reading frame encoding a predicted 106-kDa APN.

Bioinformatic Analyses of AgAPN2. The signal peptide of AgAPN2 was predicted by SignalP 3.0 (http://www.cbs.dtu.dk/services/SignalP/). Possible sites for posttranslational modification were analyzed using big-PI predictor (http://mendel.imp.ac.at/sat/gpi/gpi_server.html/) (*15−18*), Center for biological sequence prediction servers (http://www.cbs.dtu.dk/services/), and *O*-glycosylation prediction electronic tool (OGPET v1.0, http://129.108.112.23/OGPET).

Preparation of Rabbit Polyclonal Serum against an E. coli Expressed 70-kDa AgAPN2 Peptide. A central region of the AgAPN2 cDNA encoding amino acid residues 228 to 843 was amplified by PCR using the pair primer AgAPN2-F4/R4 (Table 1, Figue 1A). The PCR fragment was then cloned into the protein expression vector pET-30a (+) (Novagen, Madison, WI) and transformed into *E. coli* strain BL21-CodonPlus (DE3)/pRIL. Protein expression and purification were performed according to the pET system manual ninth edition (Novagen). The recombinant truncated APN protein, APN2$_t$, was purified by a HiTrap Ni^{2+}-chelating HP column (GE Healthcare, Piscataway, NJ) according to manufacturer's manual, dialyzed against 10 mM Tris-HCl (pH 8.0), and stored at −20 °C until needed for experimentation. APN2$_t$ peptide was used to raise antiserum by immunization of a NZW (SPF) rabbit at the Animal Resources Facility of the University of Georgia.

Anti-AgAPN2 antibody was purified by protein A Sepharose 6MB (GE Healthcare) beads using the low-salt method (*19*). The concentration of antibody was measured by Bio-Rad protein assay using bovine serum albumin (BSA) as standard (*20*).

Partial Purification and Preparation of APN from An. gambiae BBMV for Mass Spectrometry (MS) Analysis. Frozen *An. gambiae* fourth instar larvae were kindly provided by the Malaria Research and Reference Reagent Resource Center (MR4) and stored in −80 °C until use. BBMV were prepared from whole body of fourth instar larvae by $MgCl_2$ precipitation according to ref *21* and stored in aliquots at −80 °C. Protein was measured by the Bio-Rad protein assay. APN activity (*22*), a marker for brush border membranes, was enriched about 5-fold for the final BBMV preparation compared to the initial crude larval homogenate.

Sample preparation for MS analysis was as follows. Approximately 100 mg of BBMV was solubilized overnight at 4 °C in 20 mM Tris-HCl, pH 8.0, 100 mM NaCl, and 2% (w/v) 3-[(cholamidopropyl)dimethylammonio]-1-propanesulfonate (CHAPS) supplemented with 1 mM phenylmethanesulfonyl fluoride (PMSF). Subsequently, the solution was centrifuged at 39000*g* at 4 °C for 30 min. The resulting

A

AgAPN2

1   680   914   2323 2531 2904
F1   F2   F3   R3   R2   R1

682   2529
F4   R4

B

MTLAEKLALVVLVTCACAVVSTASPLDPDRYFLVEAEPRA 40
QPEDYRLNDDVWPTHYDIEIKPYLEQEGNKAQFTFDGSAK 80
ITVSTQKQNVMQIKLHMAR***MDITAWSVTR***KSDNTIIPTLP 120
QTYDQETQILTLPLSSALQANVEYVLSFTYVGNMDDDMHG 160
FYRSYYWEDGVK***VWMGSTQFQQTHARRAFPCFDEPR***FKAT 200
FQLKINHK***TQYNVYSNTAIVGTAVAEVGR***SLTTFGVTPSM 240
SSYLIAFIVAPYQINDRDGMGILARPQAQ[NQT]QYSLDVGI 280
K***LLKALEEWIDYPYASVAGMTR***MYMAAVPDFSA**GAMENWG** 320
LLT**YRE**TNILYRSDDSTSMQQHRIAAVISHE IA**HQ**WFGDL 360
VTCEWWDVTWLN**E**GFARYYQYYGTALVETEWDLDHQFVVE 400
QLQGVMQMDSLRSTHPMTHPVYTQAQTSGIFI[NIS]YNKGA 440
VMLRMMEHYLTTETFKTALRAYIKDRAFK***TTRPEDLFNAL*** 480
NRYDPNARSYMEPWTVQPGYPLVTVTSHDTGFTITQKRFL 520
VNEPDHNEQTAWPLPITFATKASEFSITRPAFYTGMTFEI 560
PMQGASDVEYFILNNQQVGYYRVNYDAILWGKISK***ALHSE*** 600
GFGGIHVLNRAQIVDDLFNLARGDVVPYGTALEILEYLK***E*** 640
ETEYAPWLAAVNGLTTLSRRIHADDEKLFTAHILDIFSKA 680
YDIVK***FQAPTATER***RIFTYMRQNVLQWACNYGHEECSK***AA*** 720
VAEFHRYHQNPSVKVHPDLR***QVVYCEGIR***KGSTEEFEFLW 760
NQYLTTNVATEQILILQGLGCVSSSELITDMLNGIASPHV 800
RSQDK***NNAFTYVINNPYTLPHVSR***YLQQNHANWAASHGSY 840
TNVASAFNNVLARLKSDSERDAISAFIESNKNILGQAAYD 880
SIK***SGLEDYETNKQFTLRNRDEIHEFLDNK***INGGAATILA 920
[NVS]MIVGLLMLVLAR

C

42059966 42063174   42089971 42093136
2R — [AgAPN5] —//— [AgAPN2PEST] ———//——— [AgAPN3] — [AgAPN4] —
          42070199 42073368   42095012 42098180

FIGURE 1: (A) Diagram of the AgAPN2 cDNA, truncated APN2$_t$ clone, and primer locations. A gray arrowhead locates the gluzincin aminopeptidase motif. (B) Deduced amino acid sequence of AgAPN2. The putative N-terminal cleavable peptide is underlined. The putative C-terminal GPI-anchor site is in boldface. The conserved gluzincin aminopeptidase motif is in boldface and underlined. The putative N-glycosylation sites are in bold boxes. Peptides identified by MS analysis are in boldface and italics. The unique peptide of AgAPN2 is in boldface, italic, and underlined. (C) Schematic representation of the APN gene cluster on chromosome 2R. Numbers indicate the position of the starting and the ending nucleotides of each gene. The gene cloned in this research is underlined.

supernatant, diluted in buffer A [20 mM Tris-HCl, pH 8.0, 0.01% (w/v) CHAPS] was separated by anion-exchange chromatography using an Acta Explorer system (GE Healthcare). Proteins were eluted with a continuous salt gradient using buffer A and buffer B [20 mM Tris-HCl, pH 8.0, 1 M NaCl, 0.01% (w/v) CHAPS]. Fractions with APN activity were pooled and resolved on SDS−12.5% PAGE. Separated proteins were detected by staining with Coomassie Blue G-250, and a duplicate gel was blotted to PVDF filter (Millipore) for probing with anti-AgAPN2 serum.

Protein bands/plugs were destained, reduced and alkylated, and digested with trypsin, and the resulting tryptic peptides were extracted for subsequent MS analysis. Specifically, plugs were washed twice with 50 mM ammonium bicarbonate/50% methanol for 20 min at room temperature. Plugs were washed with 75% acetonitrile for 20 min at room

temperature and dried at 40 °C for 10 min. Plugs were incubated in 10 mM DTT/20 mM ammonium bicarbonate at 37 °C for 1 h. The DTT solution was removed and immediately replaced with 100 mM iodoacetamide/20 mM ammonium bicarbonate and incubated at room temperature in the dark for 30 min. Plugs were washed as above and then incubated with 200 ng of sequencing grade trypsin (Promega) at 37 °C for 2 h. Peptides were extracted twice with 50% acetonitrile/0.1% TFA for 20 min at room temperature and concentrated by SpeedVac (Jouan). Approximately 25% of the resulting peptides were spotted on a matrix-assisted laser/desorption ionization (MALDI) plate using 50% saturated α-cyano-4-hydroxycinnamic acid as a matrix (Sigma).

MS Analysis. MS and MS/MS data were acquired on a 4700 Proteomics Analyzer (Applied Biosystems) using standard acquisition methods. MS/MS data were acquired in a data-dependent fashion, selecting the top 10 most intense peaks from the MS spectrum. MS spectra were calibrated using two trypsin autolysis peaks (*m/z* 1045.5 and 2211.1). MS/MS spectra were calibrated using the instrument default processing method. An *An. gambiae* protein sequence database described in ref *23* was incorporated into a licensed copy of Mascot 1.9.05 (http://www.matrixscience.com/). Mass lists were submitted to the database considering fixed cysteine carbamidomethylation and partial methionine oxidation modifications, 1 missed tryptic cleavage, and 25 ppm mass accuracy. Identifications were cross-examined using mass accuracy and molecular weight.

Phosphatidylinositol-Specific Phopholipase C (PI-PLC) Treatment and GPI-Anchor Detection. BBMV (56 mg) suspended in 3 mL of MET buffer (0.3 M mannitol, 5 mM EGTA, 20 mM Tris-HCl, pH 7.5) was incubated with 2 units of PI-PLC (Sigma) supplemented with Complete protease inhibitor cocktail (Roche, EDTA free) overnight at room temperature. The suspension was centrifuged at 16000*g* for 10 min at 5 °C, and the released proteins were recovered in the supernatant. The presence of a cleaved GPI group was detected by using polyclonal antibody against the cross-reacting determinant (CRD) of GPI-anchored proteins (kindly provided by Dr. K. Mensa-Wilmot, University of Georgia).

Cry11Ba Toxin Binding to GPI-Anchored Proteins. About 187 mg of cyanogen bromide (CNBr) activated Sepharose 6MB (Sigma) was mixed with 2 mg of Cry11Ba toxin in 2 mL of 0.1 M NaHCO$_3$ and 0.5 M NaCl, pH 9.0, at room temperature for 4 h according to the manufacturer's manual. After precipitation, the toxin−bead complex was removed from the coupling buffer and resuspended in 2 mL of 2 M ethanolamine, pH 8.0. The mixture was incubated overnight at 4 °C to saturate all remaining activated groups. After three washes with phosphate-buffered saline solution (PBS), the toxin−bead complex was mixed with the supernatant described in the section above. The mixture was incubated overnight at 4 °C with gentle rotation. After six washes with PBS buffer, the toxin−bead complex was boiled in SDS−PAGE sample buffer for 10 min, and proteins were separated by SDS−12.5% PAGE and transferred to PVDF filter for blotting experiments. The membrane was blocked with 5% skim milk (Difco, BD) in PBST (PBS + 0.1% Tween 20) for 1 h at room temperature. Then the filter was incubated with anti-AgAPN2 or anti-CRD antibody (1:2000 and 1:10000 dilution, respectively) in blocking buffer

overnight at 4 °C, washed four times, and was followed by anti-rabbit IgG horseradish peroxidase conjugate (Sigma) (1:25000 dilution) in the same buffer for 1 h at room temperature. The bound antibody was visualized by chemiluminescent substrate (ECL kit; GE Healthcare) and X-ray film.

Immunohistochemistry. *An. gambiae* fourth instar larvae were punctured in the thorax and end of the abdomen by a dissecting needle and immediately fixed with 4% paraformaldehyde in PBS for 2 h on ice, then dehydrated, embedded in plastic mixture, and sectioned. Immunodetection was according to ref *24*. The localization of AgAPN2 was detected by anti-AgAPN2 serum diluted 1:500 in blocking solution [5% (w/v) BSA, 0.2% (v/v) Tween-20 in PBS], whereas a control section was probed by preimmune serum diluted in the same solution.

Dot Blot Binding Assays. APN2$_t$ inclusion bodies were solubilized in 50 mM NaOH overnight at 37 °C and dialyzed against 50 mM Na_2CO_3, pH 10.5. CR11-MPED peptide from *An. gambiae* cadherin1 was purified as described in ref *11*. One microgram of each peptide was dotted onto a PVDF filter directly and probed with 0.125 nM ^{125}I-Cry11Ba. The toxin (1 μg) was labeled with 0.5 mCi of Na ^{125}I (PerkinElmer) using the chloramine-T method (*25*), and specific activity was 7.4 μCi/μg of input toxin. The filters were exposed to X-ray film at -80 °C for autoradiography.

Membrane Vesicle Binding Assays. Binding assays were performed as described in ref *25*. Duplicate samples of 8 μg of BBMV were incubated with increasing amounts of ^{125}I-Cry11Ba toxin in 100 μL of binding buffer (20 mM Na_2CO_3, pH 10.5, 0.15 M NaCl, 0.1% Tween-20, 1.5% BSA) for 18 h at 4 °C with shaking. Binding reactions were stopped by centrifugation and pellets washed twice with 1 mL of ice-cold binding buffer. Radioactivity of the final pellets was measured with a Beckman model Gamma 4000 detector. For homologous and heterologous competition assays, 10 μM unlabeled Cry11Ba toxin or peptides were used to compete the binding of ^{125}I-Cry11Ba toxins to BBMV. The experiments were repeated twice.

Microtiter Plate Binding Assays. A protein−protein binding assay using coated microtiter plates and enzyme-linked immunosorbent assay (ELISA) for detection was developed from the protocol of Braitbard et al. (*26*). The purified APN2$_t$ peptide was biotinylated using a 50-fold molar excess of *N*-hydroxysulfosuccinimide ester−PC−biotin (Pierce, Rockford, IL) according to the manufacturer's instructions. The final reaction was dialyzed against 20 mM Na_2CO_3, pH 9.6. Microtiter plates (high-binding, 96-well, Immulon 2HB; Thermo Fisher Scientific Inc., Waltham, MA) were coated overnight at 4 °C with 0.5 μg of Cry11Ba/well in 100 μL of coating buffer (100 mM Na_2CO_3, pH 9.6) and blocked 1 h at room temperature with PBS/0.5% BSA/0.05% Tween-20. For the binding assays, biotinylated APN2$_t$ peptide was diluted to the desired concentrations (0.001−20 nM) in 100 μL of wash buffer (PBS/0.05% Tween-20). For the competition assays, a 1000-fold molar excess of nonlabeled APN2$_t$ peptide was added into solution containing biotinylated APN2$_t$. A 100 μL aliquot of biotin−AgAPN2$_t$ solution was added to each well, and the plates were incubated at room temperature for 2 h. The plates were then washed three times, and 100 μL of horseradish peroxidase conjugated streptavidin (SA-HRP; Pierce) diluted 1:10000 in wash buffer was added

in each well. After incubation at room temperature for 1 h and washing as above, 50 μL of HRP chromogenic substrate (1-Step Ultra TMB-ELISA; Thermo Fisher Scientific Inc.) was added to detect bound SA-HRP. The reaction was stopped by the addition of 50 μL of 2 M sulfuric acid; after 5 min the absorbance at 450 nm was measured with a microplate reader (MDS Analytical Technologies, Sunnyvale, CA). Specific binding was determined by subtracting nonspecific binding from total binding. All samples were in duplicate, and the assay was repeated. Data were analyzed using SigmaPlot software (Version 11; Systat Software Inc., San Jose, CA), and the curves were fitted based on a best fit of the data to a one-site saturation binding equation.

Toxicity Bioassays. Soluble Cry11Ba was mixed with APN2$_t$ or CR11-MPED inclusion bodies at 1:100 toxin:peptide mass ratio. Cry11Ba alone or toxin−peptide mixtures were transferred to wells of a 6-well Costar culture plate (Corning). Ten early fourth instar larvae were added to each well and the plates stored at 27 °C. Each treatment was at least duplicated, and the bioassays were conducted three times, and there was a control of inclusion bodies alone. Larval mortality was recorded after 48 h.

RESULTS

Cloning AgAPN2 cDNA from the Midgut of An. gambiae Larvae. The APN$_{Anq}$100 protein purified from *An. quadrimaculatus* larvae binds Cry11Ba with high affinity and specificity (*12*). Using the reported 20 amino acid residues of the N-terminal APN sequence, we searched the *An. gambiae* whole genome sequence [Ensembl *An. gambiae* genome assembly AgamP3, February 2006 (http://www.ensembl.org/Anopheles_gambiae/ index.html)] using BLAST. The search results yielded a single predicted protein (ENSANGP00000025222) as having 85% identity to the 20 residues of APN$_{Anq}$100, and two other proteins (ENSANGP00000021245, ENSANGP00000025086) having an 80% match. These three predicted proteins matched to the three *An. gambiae* proteins specified as candidate APN$_{Anq}$100 homologues by Abdullah et al. (*12*).

We selected ENSANGP00000025222 for further analysis. Using the RT-PCR strategy shown in Figure 1A, we cloned a cDNA encoding the predicted APN from midgut tissue of *An. gambiae* larvae. The cDNA was designated *AgAPN2* (GenBank accession number EU827528), since Dinglasan et al. (*27*) had previously assigned AgAPN1 to another APN that is not one of these three and shows 20% identity to the 20 amino acid N-terminal sequence of APN$_{Anq}$100. The cloned AgAPN2 cDNA is 2904 bp long and contains a 2808 bp open reading frame. The predicted start codon is embedded in an "adequate" Kozak consensus (A<u>G</u>A<u>ATG</u>ACA) (*28*). A polyadenylation signal sequence (AATAAA) is located 83 bp downstream of the stop codon TAG. *AgAPN2* encodes a 935 amino acid protein with a theoretical molecular size of 106 kDa (Figure 1B). AgAPN2 has a 20 amino acid sequence (residues 40−59) with 85% identity to the N-terminus of mature APN$_{Anq}$100 identified previously. Analysis of the AgAPN2 protein predicts an N-terminal signal peptide, a C-terminal GPI site with ^{913}Gly as the predicted ω-site, and three *N*-glycosylation sites. AgAPN2 contains a consensus gluzincin aminopeptidase motif, **GAMENWG-X$_3$-YRE-X$_{23}$-HE-X$_2$-H-X$_{18}$-E** (where X is any amino acid) (*29*), that is associated with Zn^{2+} binding (*30*).

Table 2: Annotation of Four APN-like Genes on Chromosome 2R

genes	Ensembl identifier[a]	positions	exons	ESTs coverage (%)[b]	similarity to ESTs (%)
AgAPN2	N/A[c]	2R:42070199−42073368	6	85	>99.37
AgAPN3	18756	2R:42089971−42093136	6	84	>98.99
AgAPN4	18740	2R:42095012−42098180	6	85[d]	>98.67[d]
AgAPN5	18817	2R:42059966−42063174	6	93	>99.35

[a] ENSANGG000000, the prefix of Ensembl gene identifier is omitted. [b] Percentage of the gene squence that is supported by EST sequences deposited in GenBank ESTs (March 2008). [c] This gene has not been computationally annotated in the Ensembl database. [d] EST sequences support AgAPN2 and AgAPN4 are the same.

AgAPN2 cloned from the G3 strain corresponds to a genomic region in the PEST strain that was used for the whole genome assembly. It is noteworthy that the region has not been computationally annotated to locate the APN gene in the Ensembl *An. gambiae* genome assembly AgamP3; thus the counterpart gene of *AgAPN2* in the PEST strain was named *AgAPN2$_{PEST}$*. The genes encoding the three APN proteins mentioned above, ENSANGP00000021245, ENSANGP00000025222, and ENSANGP00000025086, are located adjacent to *AgAPN2$_{PEST}$* (Figure 1C, Table 2) and have been incorrectly combined and designated as AGAP003696 in Ensembl's release 49 (March 2008). We tentatively designate them as *AgAPN3*, *AgAPN4*, and *AgAPN5*. AgAPN2 has one amino acid substitution ($T^{884} \rightarrow S^{884}$) as compared to AgAPN2$_{PEST}$. AgAPN2 shows 99% amino acid identity to AgAPN4, 95% to AgAPN3, and 56% to AgAPN5.

Peptide Mass Fingerprinting (PMF) Identification of the 106-kDa APN Prepared from BBMV as AgAPN2. The predicted protein encoded by *AgAPN2* cDNA was correlated with an actual brush border membrane protein. An aminopeptidase-enriched protein fraction was isolated by anion-exchange chromatography from solubilized BBMV (Figure 2A). As shown in Figure 2B, anti-AgAPN2 serum specifically recognized a 106-kDa protein(s) in the enriched fraction (Figure 2B, lane 2). The 106-kDa band (Figure 2B, lane 1) was excised and digested with trypsin, and the resulting fragments were analyzed by MALDI-TOF MS. Mascot software was used to search the database (*23*) of predicted *Anopheles* proteins with the 104 peptide masses for matched proteins having significant Mascot scores greater than 58 (*p* < 0.05). The results yielded three highly similar APNs (AgAPN2$_{PEST}$, AgAPN3, and AgAPN4) that matched with high possibilities. To further determine the presence of AgAPN2 in the 106-kDa band, we examined the unique peptide(s) of AgAPN2. As shown in Figure 1B, AgAPN2 had one unique peptide matched to the observed mass, indicating that AgAPN2 was present in the 106-kDa band and recognized by anti-AgAPN2. The MALDI-TOF MS data also suggest the presence of AgAPN3 in the 106-kDa band, since three unique peptides of AgAPN3 were identified in the peptide mixture (Figure S1 in the Supporting Information).

Localization of AgAPN2 in An. gambiae in the Gut Tissue. We used immunohistochemistry with anti-AgAPN2 serum and sectioned whole larvae of *An. gambiae* to confirm that AgAPN2 is a brush border protein. The results are shown in Figure 3; AgAPN2 was localized to the posterior region of midgut on the apical portion of the brush border (i.e., microvilli). A control section probed by preimmune serum was not immunostained in the midgut region (Figure 3).
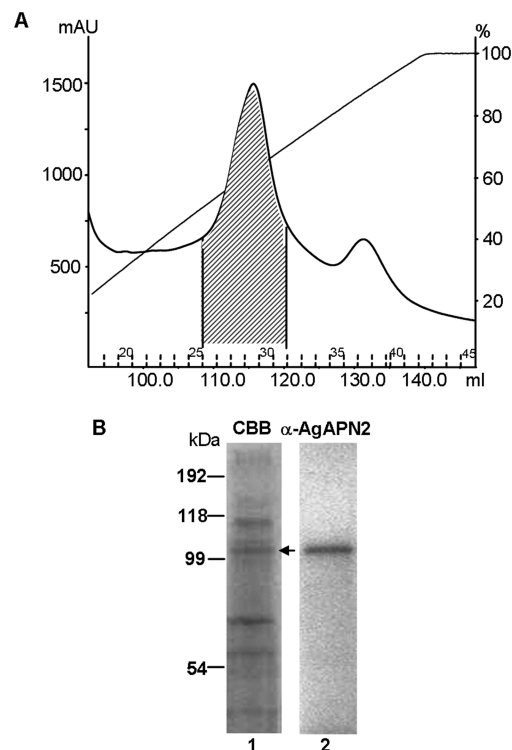

FIGURE 2: Peptide mass fingerprinting identification of a 106-kDa protein from BBMV as AgAPN2. (A) Solubilized proteins from BBMV were fractionated by 0.0−1.0 M NaCl gradient elution. The left side *Y*-axis indicates the UV absorbance at 280 nm (mAU), and the right side *Y*-axis indicates the percent conductivity of buffer B (%). Run volumes (mL) and collected fractions are indicated at the bottom. (B) Fractions 26−31 (hatched area) with APN activities were pooled and separated on SDS−PAGE. The Coomassie blue stained band at ∼100 kDa (arrowhead, lane 1) corresponds to the band recognized by anti-AgAPN2 serum on a blot (lane 2). The band was excised for mass fingerprinting.

The Affinitive Binding of Cry11Ba Toxin to GPI-Anchored AgAPN2 in BBMV. Since midgut APNs in insect larvae are typically attached to brush border membrane by GPI anchors (*22, 27, 31*), we verified the predicted anchorage of AgAPN2. BBMV were treated with PI-PLC, and strips from a blot of released proteins were probed with anti-CRD or anti-AgAPN2 antibodies. Anti-CRD antibody detects the glycan epitope on the protein's C-terminus generated by PI-PLC cleavage. The anti-CRD antibody recognized proteins ranging in size from about 20 to 118 kDa, indicating the presence and release of multiple GPI-anchored proteins from the BBMV (Figure 4A, lane 1). Anti-AgAPN2 and anti-CRD antibodies recognized a 106-kDa protein (Figure 4A, lanes 1 and 2). Since 100-kDa APN$_{Anq}$ from *An. quadrimaculatus* specifically binds Cry11Ba, we examined its homologue AgAPN2 for Cry11Ba binding. The supernatant from PI-PLC-treated BBMV was applied to the Cry11Ba toxin−bead complex, and bound proteins were examined by anti-CRD or anti-AgAPN2 antibodies. Cry11Ba precipitated three proteins including 106-kDa AgAPN2 (Figure 4B, lanes 4 and 6). The 116-kDa protein that was precipitated by Cry11Ba was tentatively identified as AgAPN1 based on cross-reactivity with anti-AgAPN1 serum (serum provided by R. Dinglasan, Johns Hopkins University; data not shown).

The Interaction of a Truncated 70-kDa AgAPN2 Peptide to Cry11Ba. We hypothesized that AgAPN2 was a specific binding protein of Cry11Ba and performed assays to
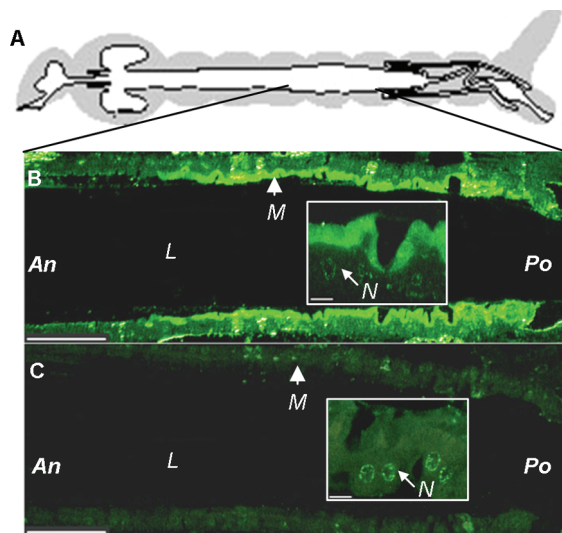
FIGURE 3: Immunolocalization of AgAPN2 on the microvilli of the posterior midgut of *An. gambiae* larvae. (A) Diagram of a mosquito gut (adapted from ref *40*). (B) Sectioned midgut was probed by anti-AgAPN2 serum and detected by Alexa Fluor-488-conjugated goat anti-rabbit IgG. (C) Control section was probed by preimmune serum. (Insets) Higher magnification views correspond to the area of apical membrane of epithelial cells in the lower magnification image. Abbreviations: *M*, microvilli; *L*, lumen; *An*, anterior; *Po*, posterior; *N*, nucleus. Scale bar: 100 and 50 μm for the low- and high-magnification images, respectively. All midgut sections were arranged anterior to the left.
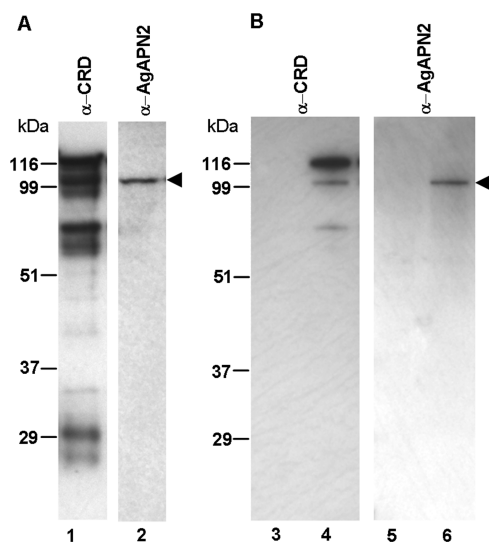
FIGURE 4: Solubilization of AgAPN2 from *An. gambiae* BBMV proteins by PI-PLC digestion and extraction with Cry11Ba beads. (A) PI-PLC-solubilized proteins were resolved by SDS–PAGE, transferred to PVDF filters, and probed with anti-CRD serum (lane 1) or anti-AgAPN2 antibody (lane 2). (B) Affinity extraction of GPI-anchored proteins with the Cry11Ba–bead complex. After being washed, the beads with bound proteins were boiled in SDS sample buffer, separated by SDS–PAGE, transferred to a PVDF filter, and then probed with anti-CRD (lanes 3 and 4) or anti-AgAPN2 antibodies (lanes 5 and 6). A GPI-anchored protein migrating at 106 kDa was extracted by Cry11Ba beads and detected by anti-AgAPN2 antibodies (arrow). Beads alone extracted no proteins (lanes 3 and 5).

investigate *in vitro* binding of Cry11Ba to AgAPN2. To circumvent difficulties in purifying AgAPN2 from larval BBMV, we attempted to produce recombinant 106-kDa AgAPN2 in *E. coli*. Since this approach was not successful, we analyzed Cry11Ba binding on a blot of the truncated 70-

kDa peptide used to raise antiserum. One microgram of purified APN2$_t$ peptide was dotted onto a PVDF membrane, and the membrane was probed with ^{125}I-labeled Cry11Ba toxin. Since the CR11-MPED peptide that originates from *An. gambiae* midgut cadherin protein was reported as a binding protein of a mosquitocidal toxin (Cry4Ba) in *An. gambiae* (*11*), purified CR11-MPED peptide was also dotted onto the membrane to test for Cry11Ba binding. The blots of each protein were probed separately. As shown in Figure 5B, Cry11Ba bound to purified 70-kDa APN2$_t$ peptide but weakly to CR11-MPED on blots.

To determine Cry11Ba specific binding, we performed homologous competition assays with increasing amounts of labeled toxin using *An. gambiae* BBMV. Under the highest concentration of toxin addition, 10 μM unlabeled Cry11Ba displaced 42% of the ^{125}I-Cry11Ba binding, reducing bound toxin from 16.9 to 9.8 fmol (Figure 5B). Thus 0.625 nM labeled Cry11Ba showed the specific binding of 0.90 pmol/mg of BBMV. To evaluate the capacity of toxin binding to AgAPN2, we performed heterologous competition assays using 10 μM APN2$_t$ or CR11-MPED peptides as competitors. For each experiment, the binding of ^{125}I-toxin was reduced from 16.9 to 11.3 or 15.0 fmol, respectively. The addition of APN2$_t$ displaced 33% of the ^{125}I-Cry11Ba binding whereas CR11-MPED only competed 11% of the binding (Figure 5B). We could not calculate K_d or K_{com} because no saturated binding was obtained for this experiment with up to 18.75 nM input ^{125}I-Cry11Ba.

The binding affinity of Cry11Ba to APN2$_t$ peptide was further analyzed by a protein−protein binding assay based on ELISA. As shown in Figure 5C, biotinylated APN2$_t$ peptide bound Cry11Ba, and the addition of 1000-fold of the unlabeled peptide competed binding. The binding curves were fit to a one-site saturation binding model, yielding a $K_d = 6.4 \pm 1.4$ nM dissociation constant for APN2$_t$ peptide binding to Cry11Ba. This indicated a strong binding of AgAPN2$_t$ to Cry11Ba.

Because the 70-kDa APN2$_t$ peptide competed the binding of Cry11Ba to larval BBMV, we predicted that this peptide would interfere with the potency of Cry11Ba against *An. gambiae*. Bioassays were used to test the effect of APN2$_t$ peptide on Cry11Ba toxicity against *An. gambiae*. Fourth instar larvae of *An. gambiae* were fed with Cry11Ba toxin alone or in combination with APN2$_t$ or CR11-MPED inclusion body. The toxicity of Cry11Ba was reduced by 98% when larvae were fed with toxin and APN2$_t$ peptide (Figure 5D). The APN2$_t$ inclusion body alone showed no toxicity to *An. gambiae* larvae (data not shown). The addition of CR11-MPED peptide reduced Cry11Ba toxicity by 29%.

DISCUSSION

In this study, we cloned cDNA of *AgAPN2* encoding a homologue of APN$_{Anq}$100 from *An. gambiae* midgut tissue and characterized AgAPN2 with respect to its localization in larval midgut and Cry11Ba interactions. Aminopeptidases function as Cry1 toxin binding proteins in a number of lepidopteran species (reviewed in ref *3*). Functional assays have demonstrated receptor function for combinations of Cry1 toxins and specific APNs in several species including tobacco hornworm (*Manduca sexta*), silkworm (*Bombyx mori*), and cotton leafworm (*Spodoptera litura*) reviewed in
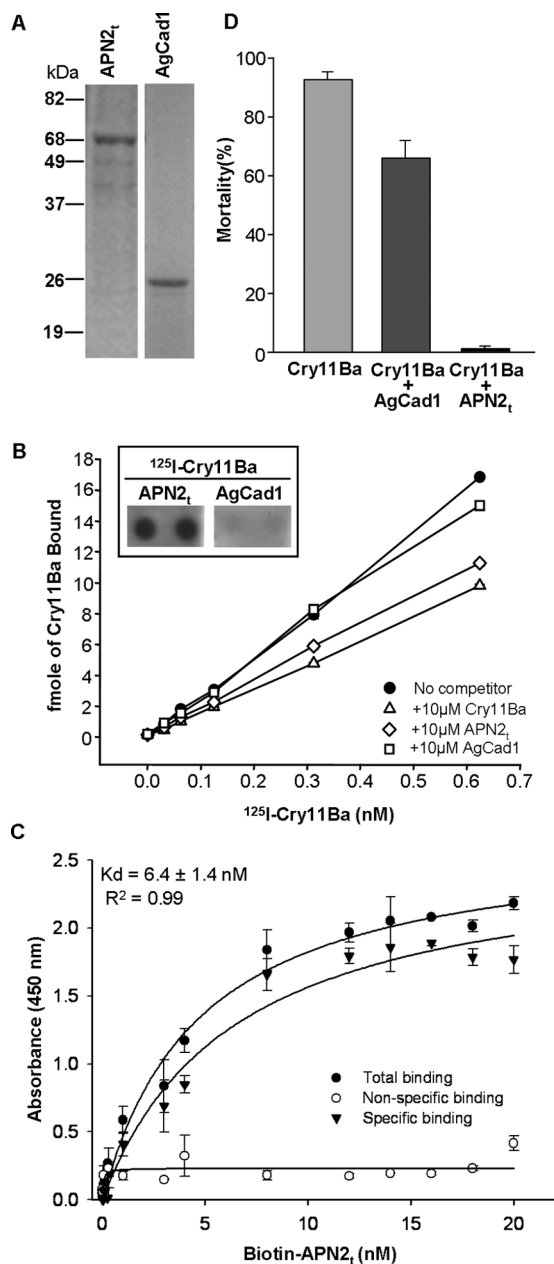
FIGURE 5: Analysis of the interaction between Cry11Ba and AgAPN2 protein. (A) Partially purified recombinant APN2$_t$ or AgCad1 CR11-MPED fragment (1 μg) was resolved by SDS−PAGE and stained with Coomassie blue. (B) Increasing amounts of ^{125}I-Cry11Ba were incubated with *An. gambiae* BBMV (8 μg) with or without 10 μM of each competitor in the binding buffer. (Inset) APN2$_t$ or AgCad1 CR11-MPED (1 μg) was spotted in duplicate on a PVDF membrane and probed with 0.125 nM ^{125}I-Cry11Ba. (C) Binding affinity of Cry11Ba to APN2$_t$. Ninety-six-well microtiter plates coated with 0.5 μg of trypsinized Cry11Ba were incubated with increasing nM concentrations of biotinylated APN2$_t$ peptide alone or with 1000-fold molar excess of un-labeled APN2$_t$ peptide to determine specific binding. (D) The 70-kDa APN2$_t$ inclusions were used for toxicity inhibition assay. Cry11Ba toxin or a mixture of Cry11Ba and APN2$_t$ or CR11-MPED (1:100 w/w) was diluted in plastic plates containing 2 mL of deionized water and tested against ten early fourth instar larvae of *An. gambiae*. Each treatment was at least in duplicate, and the bioassays were conducted three times. Larval mortality was recorded after 48 h. $P < 0.01$.

ref *3*. Recently, the 100-kDa APN (APN$_{Anq}$100) from *An. quadrimaculatus* was identified as a Cry11Ba toxin binding protein (*12*).

A phylogenetic tree of mature APN proteins was constructed by the maximum likelihood method based on 52 APN proteins from insects of Hemiptera, Coleoptera, Lepidoptera, and Diptera (Figure 6). The putative mature APN sequences were predicted by the SignalP 3.0 to remove the signal peptides. Nine distinct classes of APNs were identified, of which five classes correspond to the lepidopteran clades reported previously (*3, 32−35*) (Figure 6). Classes 6, 7, 8, and 9 are noteworthy because they are comprised of all the nonlepidopteran APNs that have not been phylogenetically characterized. AgAPN2 and its paralogues belong to the novel class 6. This class is also supported by LcAPN1 from an Australian sheep blowfly (*Lucilia cuprina*) (Figure 6). Class 7 includes AgAPN1 and an *Ae. aegypti* APN (AaAP-NRc2) that shows 37% identity to AgAPN1. Class 8 is represented by two coleopteran APNs whereas class 9 is represented by a single hemipteran APN. Interestingly, Angelucci et al. (*34*) have recently extended the lepidopteran APN proteins to nine phylogenetic clusters with the addition of APNs including HaAPN6, HaAPN7, and their orthologues from *B. mori*. Although a different neighbor-joining method was used, the relationship between these two phylogenetic classifications needs to be further examined.

In this study AgAPN2 was detected as a 106-kDa GPI-anchored protein in BBMV prepared from *An. gambiae* larvae (Figure 2). Initial identification was by cross-reactivity with anti-AgAPN2 serum on a blot, and confirmation was by peptide mass fingerprinting. Although AgAPN2 was resolved as a single band on one-dimensional SDS−PAGE, other proteins, possibly the related AgAPNs listed in Table 2, may have been present in the 106-kDa gel band. Since AgAPN3 tryptic digest peptides were detected in the 106-kDa band (Figure S1 in the Supporting Information), that paralogue was apparently present in the APN preparation. AgAPN3, also a predicted GPI-anchored protein, shares 95% amino acid identity to AgAPN2 and is probably recognized by polyclonal anti-AgAPN2 since the APN2$_t$ peptide used as an immunogen is 94% identical to the predicted AgAPN3 peptide. We lacked the information to support the presence of AgAPN4 in the 106-kDa band. Note the predicted AgAPN4 protein differs from AgAPN2 by only five amino acid residues making identification by peptide mass fingerprinting problematical (Figure S1 in the Supporting Information). The presence of multiple APN paralogues in a gene cluster may suggest that massive synthesis of APNs is needed for a rapid digestion of peptides over of a brief period of time.

In agreement with bioinformatic analyses, AgAPN2 is tethered to the membrane by a GPI anchor, as are other insect APNs (*36*). The AgAPN2 protein was localized to the microvilli in the posterior part of the midgut (Figure 3). The distribution of AgAPN2 agrees with the histochemical localization of cells secreting aminopeptidase activity reported in refs *37* and *38*, and microarray-based analyses of transcripts associated with nutrient metabolism (*39*). The localization of AgAPN2 to the posterior midgut is consistent with the role of APN as an exoenzyme that cleaves amino acids from the N-terminus facilitating uptake by amino acid transporters located in the intestinal epithelium.

Cry11Ba bound PI-PLC-released AgAPN2 in a native condition. There was specificity in the interaction as Cry11Ba affinitively precipitated AgAPN2 among the multiple PI-
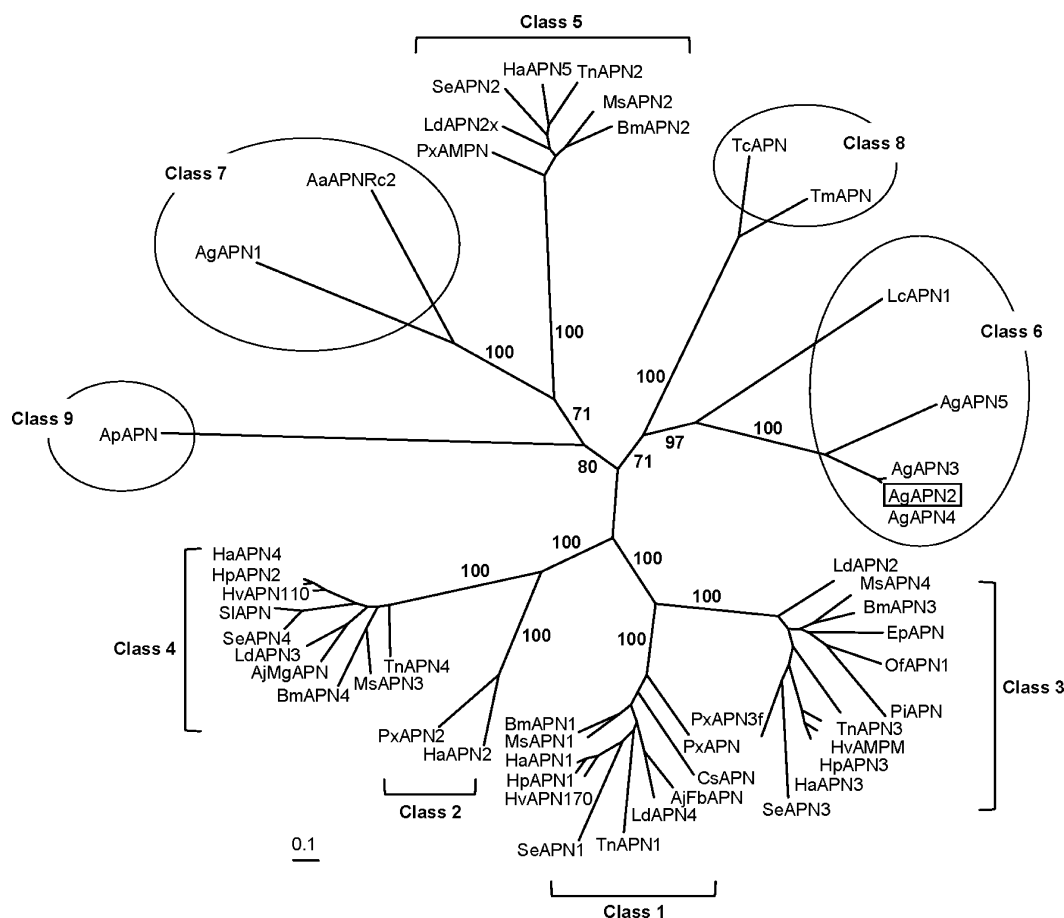
FIGURE 6: Phylogenetic tree derived from ClustalX alignment of insect APNs. The tree was constructed by the maximum likelihood method. Classifications are according to refs *3* and *31−34. GenBank accession numbers are as follows: AaAPNRc2 (AAL85580), AgAPN1(Dinglasan, personal communication), AgAPN2, AgAPN3, AgAPN4, AgAPN5 (this study), AjFbAPN (ABE02186), AjMgAPN (ABH07377), ApAPN (ABD96614), BmAPN1 (AAC33301), BmAPN2 (BAA32140), BmAPN3 (AAL83943), BmAPN4 (BAA33715), CsAPN (ABC69855), EpAPN (AAF99701), HaAPN1 (AAK85538), HaAPN2 (AAK85539), HaAPN3 (AAN04900), HaAPN4 (AAM44056), HaAPN5 (AAW72993), HpAPN1 (AAF37558), HpAPN2 (AAF37559), HpAPN3 (AAF37560), HvAPN110 (AAK58066), HvAMPM (AAC46929), HvAPN170 (AAF08254), LcAPN1 (AAM77681), LdAPN2 (AAD31183), LdAPN2x (AAD31184), LdAPN3 (AAL26894), LdAPN4 (AAL26895), MsAPN1 (CAA61452), MsAPN2 (CAA66466), MsAPN3 (AAM18718), MsAPN4 (AAM13691), OfAPN1 (ABV01346), PiAPN (AAC36148), PxAPN (AAB70755), PxAMPN (CAA66467), PxAPN2 (CAA10950), PxAPN3f (AAF01259), SeAPN1 (AAP44964), SeAPN2 (AAP44965), SeAPN3 (AAP44966), SeAPN4 (AAP44967), SlAPN (AAK69605), TcAPN (XP_972951), TmAPN (AAP94045), TnAPN1 (AAX39863), TnAPN2 (AAX39864), TnAPN3 (AAX39865), and TnAPN4 (AAX39866). Species name abbreviations are as follows: Aa, Aedes aegypti; Ag, Anopheles gambiae; Aj, Achaea janata; Ap, Acyrthosiphon pisum; Bm, Bombyx mori; Cs, Chilo suppressalis; Ep, Epiphyas postvittana; Ha, Helicoverpa armigera; Hp, Helicoverpa punctigera; Hv, Heliothis virescens; Lc, Lucilia cuprina; Ld, Lymantria dispar; Ms, Manduca sexta; Of, Ostrinia furnacalis; Pi, Plodia interpunctella; Px, Plutella xylostella; Se, Spodoptera exigua; Sl, Spodoptera litura; Tc, Tribolium castaneum; Tm, Tenebrio molitor; Tn, Trichoplusia ni. Bootstrap values represent the percentage frequency of which sequences resample in 100 replicates.*

PLC-released proteins (Figure 4). As noted in Results the 116-kDa protein visible in Figure 4 is probably AgAPN1. The precipitated 116-kDa protein seems to be more abundant than AgAPN2 or alternatively has higher affinity to Cry11Ba. We further present evidence that the peptide region (residues 228−843) of AgAPN2 binds Cry11Ba toxin. The 70-kDa truncated APN2$_t$ peptide bound the toxin on dot blot and microtiter plates (Figure 5). The binding affinity of Cry11Ba to the peptide region of AgAPN2 was determined as ca. 6.4 nM. This is comparable to a homologue of AgAPN2 (APN$_{Anq}$100) in *An. quadrimaculatus* that tightly bound Cry11Ba in the native state with a ca. 1 nM K_D (*12*). An *in vitro* competition binding assay using unlabeled Cry11Ba toxin or peptides as competitors also illustrated Cry11Ba specifically bound to *An. gambiae* BBMV. In the experiment, the 70-kDa truncated APN2$_t$ peptide competed Cry11Ba binding to BBMV, eliminating 79% of the specific binding of ^{125}I-Cry11Ba, whereas CR11-MPED from AgCad1 only competed 26% of the Cry11Ba specific binding. The ability

of AgAPN2 to compete more Cry11Ba binding on BBMV agrees with the dot blot assay, for which CR11-MPED binding to Cry11Ba was considerably less intense than that of AgAPN2. These results demonstrated AgAPN2 is a specific binding protein for Cry11Ba. The Cry11Ba specificity for a peptide region of AgAPN2 is similar to the recognition of a conserved region shared on APNs from *B. mori* that is recognized by Cry1Aa and Cry1Ab (*32*).

An *in vivo* approach was taken to correlate toxin binding to AgAPN2 with insecticidal activity. In agreement with the *in vitro* assay, when truncated AgAPN2 peptide was fed to fourth instar larvae with solubilized Cry11Ba, toxicity was reduced by 98% (Figure 5C). This inhibition is explained by Cry11Ba binding to the AgAPN2 70-kDa peptide, thereby reducing toxin binding to native AgAPN2 located on the brush border membrane. The ability of AgAPN2 to inhibit Cry11Ba toxin is evidence that Cry11Ba binding to AgAPN2 is relevant to *in vivo* toxin action.

In the Cry1A toxin−lepidopteran systems, APNs play a role with alkaline phosphatase in inserting toxin oligomers into the cell membrane (*4*). In *Ae. aegypti*, alkaline phosphatase is a functional receptor for Cry11Aa toxin (*10*). In this research, we showed that Cry11Ba bound on beads selectively extracted three proteins from BBMV proteins, including AgAPN2. Although additional research is needed to determine the relative roles of AgAPN2 and the other AgAPNs in Cry11Ba toxicity, the recognition of AgAPN2 by Cry11Ba toxin suggests that mosquitocidal Cry toxins also have a complex mode of intoxication.

ACKNOWLEDGMENT

NOTE ADDED AFTER ASAP PUBLICATION

There was an error in Figure 1 in the version published ASAP October 1, 2008; the corrected version was published ASAP October 7, 2008.

SUPPORTING INFORMATION AVAILABLE

Multiple sequence alignment of AgAPN2, AgAPN3, and AgAPN4. This material is available free of charge via the Internet at http://pubs.acs.org.

REFERENCES

1. Walker, K., and Lynch, M. (2007) Contributions of *Anopheles* larval control to malaria suppression in tropical Africa: review of achievements and potential. *Med. Vet. Entomol. 21*, 2–21.

2. Federici, B. A., Park, H. W., Bideshi, D. K., Wirth, M. C., Johnson, J. J., Sakano, Y., and Tang, M. (2007) Developing recombinant bacteria for control of mosquito larvae. *J. Am. Mosq. Control Assoc. 23*, 164–175.

3. Pigott, C. R., and Ellar, D. J. (2007) Role of receptors in *Bacillus thuringiensis* crystal toxin activity. *Microbiol. Mol. Biol. Rev. 71*, 255–281.

4. Bravo, A., Gomez, I., Conde, J., Munoz-Garay, C., Sanchez, J., Miranda, R., Zhuang, M., Gill, S. S., and Soberon, M. (2004) Oligomerization triggers binding of a *Bacillus thuringiensis* Cry1Ab pore-forming toxin to aminopeptidase N receptor leading to insertion into membrane microdomains. *Biochim. Biophys. Acta 1667*, 38–46.

5. Ravoahangimalala, O., and Charles, J. F. (1995) In vitro binding of *Bacillus thuringiensis* var. *israelensis* individual toxins to midgut cells of *Anopheles gambiae* larvae (Diptera: Culicidae). *FEBS Lett. 362*, 111–115.

6. Yamagiwa, M., Kamauchi, S., Okegawa, T., Esaki, M., Otake, K., Amachi, T., Komano, T., and Sakai, H. (2001) Binding properties of *Bacillus thuringiensis* Cry4A toxin to the apical microvilli of larval midgut of *Culex pipiens. Biosci., Biotechnol., Biochem. 65*, 2419–2427.

7. Kamauchi, S., Yamagiwa, M., Esaki, M., Otake, K., and Sakai, H. (2003) Binding properties of *Bacillus thuringiensis* Cry1C delta-endotoxin to the midgut epithelial membranes of *Culex pipiens. Biosci., Biotechnol., Biochem. 67*, 94–99.

8. Clark, T. M., Hutchinson, M. J., Huegel, K. L., Moffett, S. B., and Moffett, D. F. (2005) Additional morphological and physiological heterogeneity within the midgut of larval *Aedes aegypti* (Diptera: Culicidae) revealed by histology, electrophysiology, and effects of *Bacillus thuringiensis* endotoxin. *Tissue Cell 37*, 457–468.

9. Buzdin, A. A., Revina, L. P., Kostina, L. I., Zalunin, I. A., and Chestukhina, G. G. (2002) Interaction of 65- and 62-kD proteins from the apical membranes of the *Aedes aegypti* larvae midgut epithelium with Cry4B and Cry11A endotoxins of *Bacillus thuringiensis. Biochemistry (Moscow) 67*, 540–546.

10. Fernandez, L. E., Aimanova, K. G., Gill, S. S., Bravo, A., and Soberon, M. (2006) A GPI-anchored alkaline phosphatase is a functional midgut receptor of Cry11Aa toxin in *Aedes aegypti* larvae. *Biochem. J. 394*, 77–84.

11. Hua, G., Zhang, R., Abdullah, M. A., and Adang, M. J. (2008) *Anopheles gambiae* cadherin AgCad1 binds the Cry4Ba toxin of *Bacillus thuringiensis israelensis* and a fragment of AgCad1 synergizes toxicity. *Biochemistry 47*, 5101–5110.

12. Abdullah, M. A., Valaitis, A. P., and Dean, D. H. (2006) Identification of a *Bacillus thuringiensis* Cry11Ba toxin-binding aminopeptidase from the mosquito *Anopheles quadrimaculatus. BMC Biochem. 7*, 16.

13. Delecluse, A., Rosso, M. L., and Ragni, A. (1995) Cloning and expression of a novel toxin gene from *Bacillus thuringiensis* subsp. *jegathesan* encoding a highly mosquitocidal protein. *Appl. Environ. Microbiol. 61*, 4230–4235.

14. Schaeffer, P., Millet, J., and Aubert, J. P. (1965) Catabolic repression of bacterial sporulation. *Proc. Natl. Acad. Sci. U.S.A. 54*, 704–711.

15. Eisenhaber, B., Bork, P., and Eisenhaber, F. (1998) Sequence properties of GPI-anchored proteins near the omega-site: constraints for the polypeptide binding site of the putative transamidase. *Protein Eng. 11*, 1155–1161.

16. Eisenhaber, B., Bork, P., and Eisenhaber, F. (1999) Prediction of potential GPI-modification sites in proprotein sequences. *J. Mol. Biol. 292*, 741–758.

17. Sunyaev, S. R., Eisenhaber, F., Rodchenkov, I. V., Eisenhaber, B., Tumanyan, V. G., and Kuznetsov, E. N. (1999) PSIC: profile extraction from sequence alignments with position-specific counts of independent observations. *Protein Eng. 12*, 387–394.

18. Eisenhaber, B., Bork, P., Yuan, Y., Loffler, G., and Eisenhaber, F. (2000) Automated annotation of GPI anchor sites: case study *C. elegans. Trends Biochem. Sci. 25*, 340–341.

19. Harlow, E., and Lane, D. (1988) Storing and purifying antibodies, in *Antibodies: A Laboratory Manual*, 1st ed., p 310, Cold Spring Harbor Laboratory Press, New York.

20. Bradford, M. (1976) A rapid and sensitive method for the quantitation of microgram quantities of protein utilizing the principle of protein-dye binding. *Anal. Biochem. 72*, 248–254.

21. Silva-Filha, M. H., Nielsen-Leroux, C., and Charles, J.-F. (1997) Binding kinetics of *Bacillus sphaericus* binary toxin to midgut brush-border membranes of *Anopheles* and *Culex* sp. mosquito larvae. *Eur. J. Biochem. 247*, 754–761.

22. Garczynski, S. F., and Adang, M. J. (1995) Bacillus thuringiensis CryIA(c) δ-endotoxin binding aminopeptidase in the *Manduca sexta* midgut has a glycosyl-phosphatidylinositol anchor. *Insect Biochem. Mol. Biol. 25*, 409–415.

23. He, N., Botelho, J. M. C., McNall, R. J., Belozerov, V., Dunn, W. A., Mize, T., Orlando, R., and Willis, J. H. (2007) Proteomic analysis of cast cuticles from *Anopheles gambiae* by tandem mass spectrometry. *Insect Biochem. Mol. Biol. 37*, 135–146.

24. Chen, J., Brown, M. R., Hua, G., and Adang, M. J. (2005) Comparison of the localization of *Bacillus thuringiensis* Cry1A delta-endotoxins and their binding proteins in larval midgut of tobacco hornworm *Manduca sexta. Cell Tissue Res. 321*, 123–129.

25. Garczynski, S. F., Crim, J. W., and Adang, M. J. (1991) Identification of putative insect brush border membrane-binding molecules specific to *Bacillus thuringiensis* delta-endotoxin by protein blot analysis. *Appl. Environ. Microbiol. 57*, 2816–2820.

26. Braitbard, O., Glickstein, H., Bishara-Shieban, J., Pace, U., and Stein, W. D. (2006) Competition between bound and free peptides in an ELISA-based procedure that assays peptides derived from protein digests. *Proteome Sci. 4*, 12.

27. Dinglasan, R. R., Kalume, D. E., Kanzok, S. M., Ghosh, A. K., Muratova, O., Pandey, A., and Jacobs-Lorena, M. (2007) Disruption of *Plasmodium falciparum* development by antibodies against a conserved mosquito midgut antigen. *Proc. Natl. Acad. Sci. U.S.A. 104*, 13461–13466.

28. Kozak, M. (1987) An analysis of 5′-noncoding sequences from 699 vertebrate messenger RNAs. *Nucleic Acids Res. 15*, 8125–8148.

29. Laustsen, P. G., Rasmussen, T. E., Petersen, K., Pedraza-Diaz, S., Moestrup, S. K., Gliemann, J., Sottrup-Jensen, L., and Kristensen,

T. (1997) The complete amino acid sequence of human placental oxytocinase. *Biochim. Biophys. Acta 1352*, 1–7.

30. Hooper, N. M. (1994) Families of zinc metalloproteases. *FEBS Lett. 354*, 1–6.

31. Takesue, S., Yokota, K., Miyajima, s., Taguchi, R., and Ikezawa, H., and Takesue, Y. (1992) Partial release of aminopeptidase N from larval midgut cell membranes of the silkworm, *Bombyx mori*, by phosphatidylinositol-specific phospholipase C. *Comp. Biochem. Physiol. 102B*, 7–11.

32. Nakanishi, K., Yaoi, K., Nagino, Y., Hara, H., Kitami, M., Atsumi, S., Miura, N., and Sato, R. (2002) Aminopeptidase N isoforms from the midgut of *Bombyx mori* and *Plutella xylostella*—their classification and the factors that determine their binding specificity to *Bacillus thuringiensis* Cry1A toxin. *FEBS Lett. 519*, 215–220.

33. Herrero, S., Gechev, T., Bakker, P. L., Moar, W. J., and de Maagd, R. A. (2005) *Bacillus thuringiensis* Cry1Ca-resistant *Spodoptera exigua* lacks expression of one of four aminopeptiase N genes. *BMC Genomics 6*, 96.

34. Wang, P., Zhang, X., and Zhang, J. (2005) Molecular characterization of four midgut aminopeptidase N isozymes from the cabbage looper *Trichoplusia ni*. *Insect Biochem. Mol. Biol. 6*, 611–620.

35. Angelucci, C., Barrett-Wilt, G. A., Hunt, D. F., Akhurst, R. J., East, P. D., Gordon, K. H. J., and Campbell, P. M. (2008) Diversity of aminopeptidases, derived from four lepidopteran gene duplications, and polycalins expressed in the midgut of *Helicoverpa armigera*: Identification of proteins binding the δ-endotoxin, Cry1Ac of *Bacillus thuringiensis*. *Insect Biochem. Mol. Biol. 38*, 685–696.

36. Adang, M. J. (2004) Insect aminopeptidase N, in *Handbook of Proteolytic Enzymes* (Barrett, A. J., Rawlings, N. D., and Woessner, J. F., Eds.) 2nd ed., Elsevier, Amsterdam.

37. Volkmann, A., and Peters, W. (1989) Investigations on the midgut caeca of mosquito larvae—I. Fine structure. *Tissue Cell 21*, 243–251.

38. Volkmann, A., and Peters, W. (1989) Investigations on the midgut caeca of mosquito larvae—II. Functional aspects. *Tissue Cell 21*, 253–261.

39. Neira Oviedo, M., Vanekeris, L., Corena-McLeod, M. D., and Linser, P. J. (2008) A microarray-based analysis of transcriptional compartmentalization in the alimentary canal of *Anopheles gambiae* (Diptera: Culicidae) larvae. *Insect Mol. Biol. 17*, 61–72.

40. Boudko, D. Y., Moroz, L. L., Linser, P. J., Trimarchi, J. R., Smith, P. J., and Harvey, W. R. (2001) In situ analysis of pH gradients in mosquito larvae using non-invasive, self-referencing, pH-sensitive microelectrodes. *J. Exp. Biol. 204*, 691–699.